The Journal of Physical Chemistry A

 VOLUME 101, NUMBER 35, AUGUST 28, 1997

LETTERS

Using Vector Correlation To Probe the Influence of Vibrational State Selection on the Photodissociation Dynamics of HN_3

Rhett James Barnes, Adam Gross, Michael Lock, and Amitabha Sinha*

Department of Chemistry and Biochemistry, University of California—San Diego, 9500 Gilman Drive, La Jolla, California 92093-0314

Received: November 4, 1996; In Final Form: June 24, 1997[⊗]

State-selected photodissociation of hydrozoic acid is investigated by vibrationally exciting the molecule in the region of the second overtone of its N−H stretching motion ($3\nu_1$) and then photodissociating it using 532 nm light. Measurement of the resulting NH fragment rotational state distribution and vector correlation reveals that photodissociation from initial nuclear configurations with an extended N−H bond leads to a substantially hotter rotational state distribution as well as a more pronounced $\langle\vec{v},\vec{j}\rangle$ correlation than from nearly isoenergetic single-photon dissociation at 355 nm. These observations are interpreted as indicating that the region of the excited electronic surface accessed and hence the forces experienced by the molecule are different in the two isoenergetic photodissociation experiments.

I. Introduction

Photodissociation experiments that combine state-selected preparation of reagents with quantum state resolved detection of products allow the most detailed probe of the dissociation dynamics and the best opportunity for unraveling the factors that control the photochemistry of a molecule. State selection resulting from vibrational excitation, for example, provides the means for probing the influence of initial nuclear motion on the photodissociation dynamics.[1]

In order to explore the influence of vibrational excitation, most recent studies have focused on comparing nascent product state distributions and quantum yields obtained from the two-step vibrationally mediated photodissociation (VMP) process with those from isoenergetic single-photon dissociation from the vibrationless ground state. However, in addition to these scalar attributes, one can also measure various vector properties characterizing the dissociation process.[2,3] Although the application of vector correlation for studying the photodissocition dynamics of vibrationally excited molecules has been limited, the experiments of Brourard et. al. on HOOH[4] and those of Rosenwaks and co-workers on H_2O[5] clearly demonstrate the feasibility of this approach. Because initial vibrational excitation allows the molecule to explore regions of the excited state potential energy surface that are distinct from those accessed via isoenergetic single-photon dissociation, the forces that the molecule experiences in a vibrationally mediated photodissociation process are likely to be different from those it experiences through direct single-photon excitation at the same total energy. These differences can be revealed using vector correlation techniques.

In this Letter we present results on the vibrationally mediated photodissociation of hydrozoic acid (HN_3) from the second overtone of the N−H stretching vibration ($3\nu_1$) using 532 nm light (see Figure 1a). We infer the influence of initial vibrational state selection by probing the resulting NH fragments using laser-induced fluorescence combined with sub-Doppler spectroscopy and by comparing the results of the $3\nu_1 + 532$ nm

[⊗] Abstract published in *Advance ACS Abstracts*, August 15, 1997.

S1089-5639(96)03440-8 CCC: $14.00

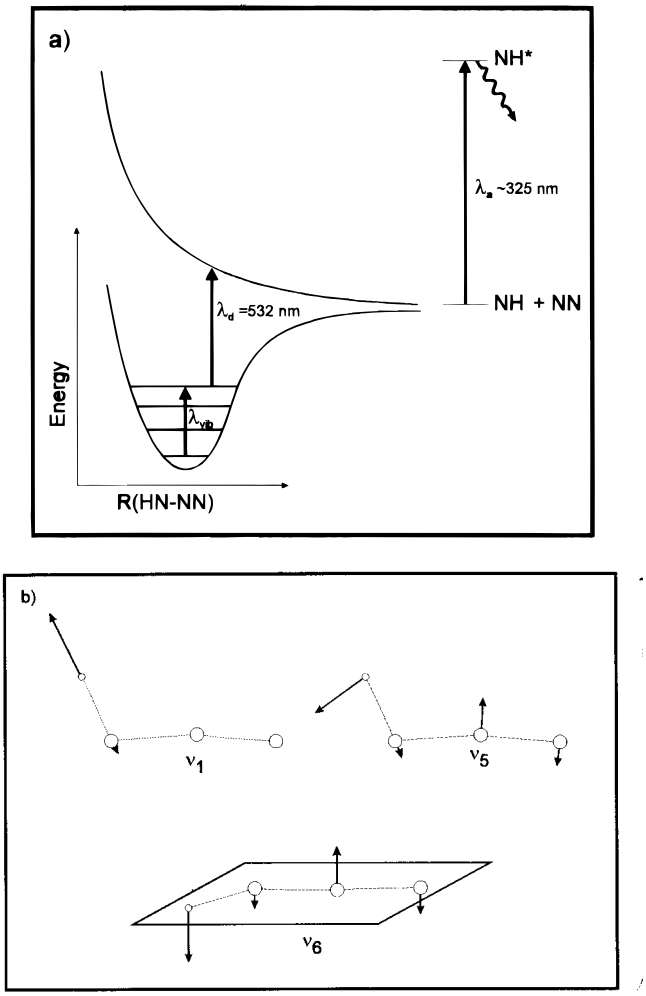

Figure 1. (a) Schematic figure illustrating the state-selected photodissociation of HN_3. (b) Some of the relevant normal modes of HN_3. The mode ν_1 corresponds to N−H stretching motion, while ν_5 and ν_6 correspond, respectively, to in-plane and out-of-plane motion of the N_3 frame.

vibrationally mediated photodissociation experiments with those from nearly isoenergetic single-photon dissociation using 355 nm light.

In many ways the HN_3 molecule is an ideal system for investigating vibrationally mediated photodissociation. Its single-photon dissociation dynamics has been studied extensively at several different UV wavelengths,[6−11] its vibrational spectroscopy is well characterized,[12−14] and even its unimolecular decomposition has been investigated.[15] In addition, several theoretical studies have been reported on HN_3 that address various aspects of the topology of its ground and low lying excited electronic potential energy surfaces.[16,17] *Ab-initio* calculations by Meier and Staemmler[17] show that for UV photolysis wavelengths longer than 220 nm the lowest excited singlet electronic surface, the $1^1A''$ state, controls the photochemistry of HN_3. This study reveals that electronic transition to the $1^1A''$ state involves the promotion of an electron from a nonbonding π orbital to an antibonding π^* orbital localized on the N_3 moiety. In addition the calculations show that although HN_3 is planar in its ground state, with the N_3 frame being nearly linear, excitation to the $1^1A''$ state results in a distortion of the molecule resulting from simultaneous excitation of both in-plane and out-of-plane bending vibrations of the NNN frame (i.e. ν_5 and ν_6; see Figure 1b). Single-photon photodissociation experiments on HN_3 at 248,[6,10] 266,[7] 283,[8] and 308 nm[7] find that the dominant product channel is N_2 ($X^1\Sigma_g$) + NH($a^1\Delta$), although a minor channel involving H + N_3 has also been observed at 248 nm.[11] In line with the theoretical predictions, rotational state distributions and vector correlation measurements on both the NH and N_2 fragments find large rotational excitation of the N_2 product but only modest internal excitation of the NH fragment, consistent with distortion of the N_3 frame upon promotion to the $1^1A''$ state.[7,8,10] It is also clear from the single-photon UV dissociation studies that varying the energy of the dissociation photon over a wide range from 308 to 248 nm has little effect on the NH($v = 0$, $a^1\Delta$) rotational state distribution, with the increased available energy being primarily channeled into internal excitation of the N_2 fragment and relative translation.[7,8,10] The invariance of the NH product rotational state distributions with photolysis wavelength over the 308−248 nm range is in agreement with the calculations of Meier and Staemmler,[17] which indicate that in the Franck−Condon region the $1^1A''$ surface does not vary appreciably with H−N−N bending angle.

Although they are able to account for a large part of the photochemistry of HN_3, it is worth noting that the calculations of Meier and Staemmler[17] fix the N−H bond length to its ground state equilibrium value. Thus the resulting surface cannot describe the dependence of the $1^1A''$ state on the N−H stretching coordinate. In this study we explore the extent to which the N−H stretching coordinate influences the photochemistry of HN_3 by preparing an initial state containing a significant amount of N−H stretching motion and investigating its influence on the photodissociation dynamics. In particular we show that photodissociation from initial configurations with an extended N−H bond leads to a substantially hotter NH fragment rotational state distribution as well as a more pronounced $\langle\vec{v},\vec{j}\rangle$ correlation compared to single-photon dissociation at roughly the same total energy.

II. Experimental Approach

The experimental apparatus is similar to that described in our earlier work on HO_2 and HOBr.[18] We generate hydrozoic acid by mixing powdered stearic acid with sodium azide in roughly a 3:1 ratio. The mixture is then transfered to a 250 mL glass round bottom flask, and the contents are heated to 80−90 °C by immersing the flask into a heated water bath.[7,9] The HN_3 generated upon heating is continuously flowed into the reaction cell which is evacuated by a partially throttled mechanical vacuum pump resulting in a total pressure in the cell of ~80 mTorr.

Vibrational overtone excitation light is generated by an Optical Parametric Oscillator (OPO, Spectra Physics MOPO-730), which is pumped by the third harmonic of a Nd:Yag laser (Spectra Physics GCR-270). The idler beam from the OPO provides continuously tunable radiation from 800 to 1800 nm with a bandwidth of ~0.4 cm^{-1} and pulse energies around 11 mJ in the wavelength region of interest. Photolysis light used to dissociate the vibrationally excited molecules is produced by the second harmonic (532 nm, 20 mJ) of another Nd:Yag laser. The polarization states of the vibrational excitation and photolysis lasers are controlled by passing the respective beams through a double Fresnel Rohmb and a prism assembly. The IR light for vibrational excitation is finally combined with the 532 nm photolysis light using a dichroic beam splitter, and the combined beams are directed into the cell after passing through a 400 mm focal length lens. For the isoenergetic single-photon dissociation studies, the third harmonic (355 nm, 1 mJ) of the photolysis Nd:Yag laser provides the necessary photons.

We probe the NH photofragments using laser-induced fluorescence via the $c^1\Pi-a^1\Delta$ transition at ~325 nm. The

probe photons are generated by frequency doubling the output of a third Nd:Yag laser (Continuum NY81-20) pumped dye laser (Continuum ND60), and its intensity is greatly attenuated in order to avoid saturation of the NH transitions. The probe laser light is passed through a Glan-Thompson polarizer to clean up its polarization. Typically, the time delay between the probe and photolysis lasers is set around 30 ns while that between the photolysis and vibrational excitation lasers is kept at 50 ns. The fluorescence excited by the probe laser is collected by an f/1 lens system and imaged onto an endon photomultiplier tube (EMI 9635QB). The combination of a colored glass filter (Corning 7-54) and an interference filter (Acton Research 310-S-SD) located in front of the photomultiplier allows us to discriminate against scattered laser light.

III. Results and Discussion

We examine the influence of vibrational excitation on the photodissociation dynamics of HN_3 using three types of measurements. In the first, monitoring a particular ro-vibrational quantum state of the NH fragment while varying the wavelength of the vibrational excitation laser generates an "action" spectrum of those HN_3 molecules that dissociate to produce fragments in the interrogated quantum state. In the second, varying the probe laser wavelength with the vibrational excitation laser fixed on a particular ro-vibrational transition of HN_3 yields an NH laser-induced fluorescence excitation spectrum from which we extract the nascent distribution of products among their quantum states. Finally, an analysis of how the Doppler profiles of the NH fragments vary as a function of the rotational branch as well as the relative propagation and polarization directions of the excitation and LIF probe lasers provides information regarding the presence of vector correlations associated with the dissociation process.

Figure 2(a) shows a vibrational overtone action spectrum of HN_3 generated by monitoring the Q(4) transition of the NH fragment while scanning the vibrational excitation laser over the spectral region corresponding to the $2\nu_1 + \nu_4$ and $3\nu_1$ bands. This medium resolution, $\sim$0.4 cm^{-1}, overtone action spectrum agrees fairly well with previously reported photoacoustic measurements of Halligan over the same spectral region.[14] Although we do not present the results here, our ability to access the ν_4 vibration, which consists of almost equal mixtures of HNN bend and HN$-$NN stretching motions,[13] allows us to examine the influence of the bending coordinate on the dissociation dynamics as well.

The NH rotational state distribution resulting from the $3\nu_1$ + 532 nm VMP experiments is shown in Figure 2b, and Table 1 summarizes the corresponding energy disposal data. The particular distribution shown in Figure 2b arises from excitation of spectral feature(s) in the region indicated by the arrow in Figure 2a. In these room temperature measurements, rotational congestion combined with our modest laser resolution precludes excitation of a single rotational quantum state of HN_3.

As in the single-photon UV photodissociation experiments at 308, 266, and 248 nm, we find that the VMP process produces NH fragments almost exclusively in the $^1\Delta$ electronic state. This observation is consistent with excitation to the $1^1A''$ state followed by spin-conserved dissociation. Surprisingly, as in the photodissociation of HN_3 from its vibrational ground state,[9,10] we also do not observe any vibrationally excited NH fragments in these VMP experiments. For comparison purposes, Figure 2b also shows the rotational state distribution resulting from single-photon dissociation at 355 nm, which is nearly isoenergetic with the $3\nu_1$ + 532 VMP experiment. We find that excitation at different points within the rotational envelope of the $3\nu_1$ band has no observable effect on the NH fragment rotational state distribution. This observation is consistent with findings from earlier single-photon UV photodissociation studies which indicate that the NH fragment rotational state distribution and vector correlations are insensitive to whether HN_3 is photodissociated at room temperature or after cooling in a supersonic expansion.[10] As is evident from Figure 2b, vibrationally mediated photodissociation of HN_3 from the $3\nu_1$ level results in a NH rotational state distribution that is noticeably hotter than that from direct single-photon dissociation. In fact, as Table 1 illustrates, comparing the current VMP data with rotational state distributions arising from single-photon dissociation using wavelengths much shorter than 355 nm (e.g.,

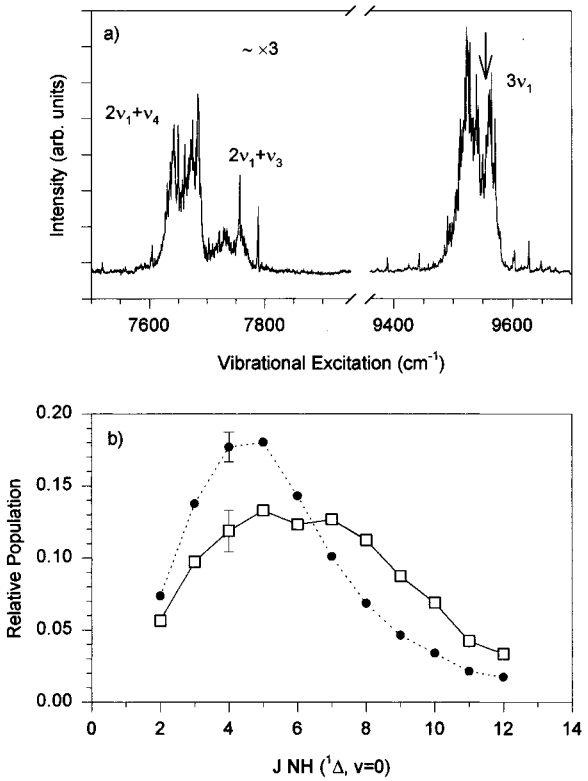

Figure 2. (a) Action spectrum generated by monitoring the NH(N = 4, v = 0, a$^1\Delta$) state as the vibrational excitation laser is scanned over the region of the $3\nu_1$ and $2\nu_1 + \nu_4$ bands. The intensity scale for the $2\nu_1 + \nu_4$ band spectral region is magnified by a factor of 3. The arrow in the figure indicates the spectral region at which the product state distribution shown below was taken. (b) Rotational product state distributions of the NH(v = 0, a$^1\Delta$) fragment resulting from the $3\nu_1$ + 532 nm VMP (squares) and single-photon 355 nm photodissociation (circles) experiments. For both experiments, the distributions were obtained by analyzing Q-branch transitions.

TABLE 1: Average Energy Disposal Data for the NH Fragment

experiment	E_{avail}[a]	E_{rot}(NH, v = 0, a$^1\Delta$)[a]	E_{trans}(NH, v = 0, a$^1\Delta$)[a]
$3\nu_1$ + 532 nm	9 720[b]	790	4530[c]
355 nm	9 820[b]	570	5340[c]
308 nm[d]	14 100	690	6950
283 nm[e]	16 970	700	6430
266 nm[d]	19 210	700	7040
248 nm[d]	21 950	700	6800

[a] All energies are in cm^{-1}. [b] $E_{avail} = h\nu + E_{int}(HN_3) - D_0$. For 355 nm photolysis we use $E_{int}(HN_3$, thermal sample) = 380 cm^{-1}, while for the VMP measurement $E_{int}(HN_3, 3\nu_1)$ = 9670 cm^{-1}. D_0 = 18 750 cm^{-1} for the dissociation channel $HN_3 \rightarrow NH(^1\Delta) + N_2(^1\Sigma)$ (ref 10). [c] Obtained by applying the procedure outined in ref 3 with a Gaussian convolution function having a fwhm of 0.13 cm^{-1}. [d] Data from ref 10. [e] Data from ref 8.

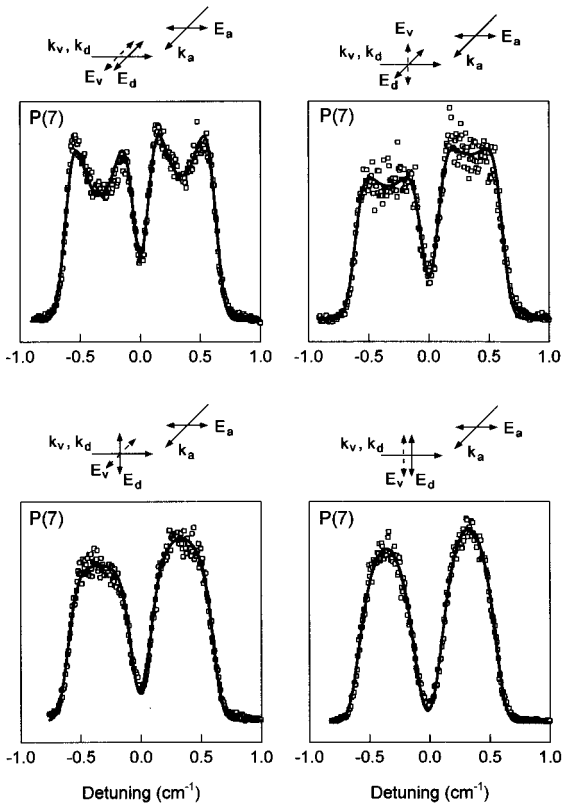

Figure 3. Variation in the NH($N = 7$, $v = 0$, $a^1\Delta$) Doppler profile as a function of the polarization/propagation direction of the excitation lasers in the $3\nu_1 + 532$ nm VMP measurements. The two primary features appearing in the Doppler profiles, separated by $\sim$0.8 cm^{-1}, correspond to the two λ-doublets components for the $N = 7$ rotational state. The vibrational excitation laser and photolysis laser propagate collinearly in these measurements. A comparison of Doppler profiles in the same row reveals how they vary with the polarization of the vibrational excitation laser. The dots are experimental points and the solid line are fits to the data using the procedure outlined in ref 3, which assumes that the parent molecules are isotropically distributed.

either 308, 266, or even 248 nm),[10] where the total available energy is significantly larger, also shows that the rotational state distributions obtained through VMP are hotter than that from direct single-photon dissociation.

The observed differences in NH rotational state distributions arising from the $3\nu_1 + 532$ nm VMP experiments versus direct 355 nm dissociation suggest that projecting the molecule onto the upper electronic state surface from extended N−H nuclear configurations allows access to different regions of the upper state surface, which in turn lead to different forces experienced by the molecule. In principle, we can obtain insight into the nature of these forces by examining the corresponding Doppler profiles. However, as is well-known, initial state preparation using polarized light can lead to an alignment of the sample.[19] Consequently, the deconvolution procedure necessary for extracting the bipolar moments from the Doppler profiles in these state selected experiments are not the same as those used to examine photodissociation of an isotropic sample.[3] The fact that the vibrational excitation laser introduces a certain degree of alignment of the parent molecule and that this in turn influences the NH Doppler profiles is readily seen from Figure 3 where we notice that for the NH($N = 7$) rotational state changing the polarization of the vibrational excitation laser while keeping the polarization and propagation directions of the photolysis and probe lasers fixed changes the shape of the Doppler profiles in the $3\nu_1 + 532$ nm VMP experiments. It is worth noting that the two primary features appearing in the Doppler profiles in Figure 3 (separated by $\sim$0.8 cm^{-1}) correspond to the two λ-doublet components for the $N = 7$ rotational state. The solid lines through the data points are fits using the procedure outlined in ref 3 *that assumes that the parent molecule is distributed isotropically*. We point out that even though the fits are reasonable and provide an estimate of the translational energy release, the interpretation of the resulting bipolar moments in terms of their original definition[3] is lost due to contributions to the data from terms that are higher order than the canonical second-order Legendre polynomial $P_2(\theta)$. These terms are required to take proper account of the observed alignment but are not included in our fitting procedure.

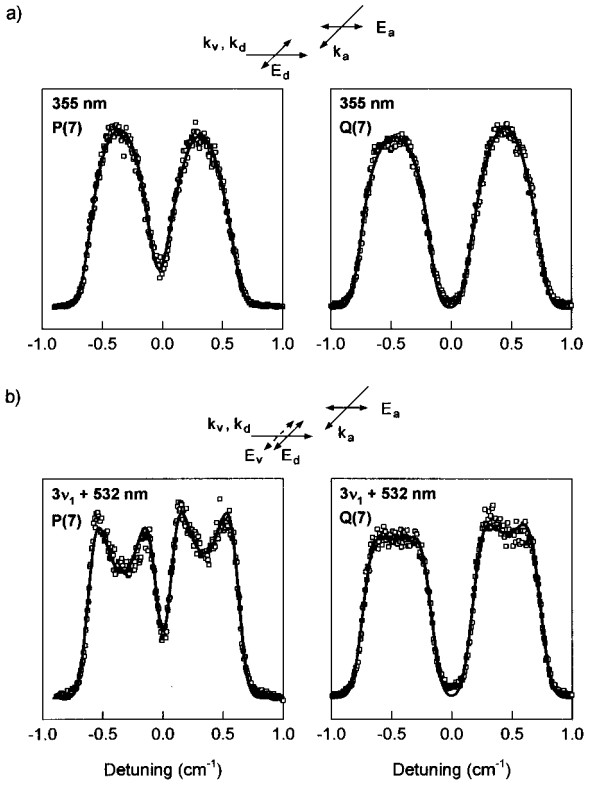

Figure 4. (a) Variation in the NH($N = 7$, $v = 0$, $a^1\Delta$) Doppler profile with rotational branch resulting from single-photon dissociation at 355 nm. The geometry for the experiment, shown above, is the same for both rotational branchs. (b) Variation in the NH($N = 7$, $a^1\Delta$) Doppler profile with rotational branch for the isoenergetic $3\nu_1 + 532$ nm VMP experiment. Again, the geometry for the experiment is the same for both rotational branches considered. In these experiments the IR laser is fixed in the spectral region indicated by the arrow in Figure 2a.

Although the presence of parent alignment currently prevents us from extracting quantitative information regarding the bipolar moments, we can still obtain a qualitative understanding of how the $\langle\vec{v},\vec{j}\rangle$ correlation varies between the two isoenergetic experiments by simply considering the changes in the NH Doppler profiles that result as we vary the probed rotational branch (P vs Q) while keeping all other aspects of the experimental geometry unchanged. Figure 4a shows the Doppler profile of the NH($N = 7$) rotational state resulting from 355 nm photolysis and its dependence on the probed rotational branch (P vs Q) for a fixed polarization/propagation geometry of the photolysis and probe lasers. The slight differences appearing between the line shapes of the P and Q branch profiles, recorded under identical geometries, indicates the presence of a weak $\langle\vec{v},\vec{j}\rangle$ correlation. A quantitative deconvolution of the Doppler profiles using the analysis outlined in ref 3 gives a value for the bipolar moment characterizing this correlation of $\beta_{vj} = 0.18$.[20] The small but positive value of this parameter indicates a slight preference for the NH fragment's $\vec{v}$ and $\vec{j}$ vectors to point parallel to one another.

Figure 4b shows the corresponding line shapes of the NH($N = 7$) state arising from the isoenergetic $3\nu_1 + 532$ nm VMP experiments probed respectively via the P and Q branches. The large variation between the line shapes of these two profiles, taken under identical geometries, as compared to the relatively modest variation seen in Figure 4a, clearly indicates that photodissociation from the $3\nu_1$ level results in substantially greater $\langle\vec{v},\vec{j}\rangle$ correlation with both vectors tending to align themselves in a much more collinear fashion than in the direct 355 nm photodissociation experiment. Thus we see that although the two photodissociation experiments correspond to similar total energies, excitation from initial nuclear configuration with an extended N−H bond apparently generates much larger torsional forces, which tend to align the fragment's rotational angular momentum and recoil velocity vectors in a collinear fashion.

We believe that the differences in the torsional forces experienced by the molecule in the two experiments results from variation in the region of the excited state surface accesed by them. Furthermore since *ab-initio* calculations[17] find only one singlet state ($1^1A''$) in this wavelength region, the differences in the two isoenergetic measurements most likely arise from excitation of the parent molecule to different regions of the *same* electronic surface and not from accessing different excited electronic states in the two experiments. We rule out the posibility that the enhanced torsional forces observed in the VMP experiment result from vibrational state mixing in the intermediate state. The rationale for this assertion is that the vibrational density of states in the energy region of the $3\nu_1$ level is low (1.3 state/cm^{-1}) and, on the basis of studies of the higher N−H stretching overtones,[15] the typical magnitude of any coupling matrix element is expected to be on the order of ∼0.1 cm^{-1}; thus, the $3\nu_1$ level is expected to be a fairly isolated stretching state. The spectral analysis of Carlotti et. al.[12] at medium resolution appears to support this notion, and although their analysis reveals local perturbations in the spectra of the $3\nu_1$ level involving rotational states of the $K_a = 2$ and $K_a = 4$ stacks the other K stacks appear to be clean. In the present experiment the 0.4 cm^{-1} resolution of the IR laser results in the excitation of a range of rotational transitions within the $3\nu_1$ level. Simulations using an asymmetric rotor fitting program however, show that in the spectral region of interest (indicated by arrow in Figure 2a) most of the intensity arises from transitions involving $K_a = 0$ and $K_a = 1$ stacks with smaller contribution coming from transitions belonging to the $K_a = 2$ and $K_a = 3$ levels. As a result of these considerations, we expect the initially prepared intermediate state to be of predominately N−H stretching charecter and the enhanced torsional motion observed in the VMP experiment to be generated in the excited electronic state. Further experiments using a higher resolution IR laser are planned to test these ideas.

Acknowledgment. Acknowledgment is made to the Academic Senate of the University of California for the partial support of this research. In addition, we thank the National Science Foundation for support of this work. The authors thank Priv.-Doz. Dr. K.-H. Gericke for making available the *b*-multiplier coefficients used to simulate the NH Doppler profiles and Prof. Joe Francisco for help with the normal mode analysis.

References and Notes

(1) Crim, F. F. *Annu. Rev. Phys. Chem.* **1993**, *44*, 397.

(2) (a) Houston, P. L. *J. Phys. Chem.* **1987**, *91*, 5388. (b) Hall, G. E.; Houston, P. L. *Annu. Rev. Phys. Chem.* **1989**, *40*, 375.

(3) Dixon, R. N. *J. Chem. Phys.* **1986**, *85*, 1866.

(4) (a) Brourard, M.; Martinez, M. T.; O'Mahony, J.; Simons, J. P. *Chem. Phys. Lett.* **1988**, *150*, 6. (b) Brourard, M.; Martinez, M. T.; O'Mahony, J.; Simons, J. P. *J. Chem. Soc., Faraday Trans. 2* **1989**, *85*, 1207. (c) Brourard, M.; Martinez, M. T.; O'Mahony, J.; Simons, J. P. *Mol. Phys.* **1990**, *69*, 65. (d) Brouard M.; Mabbs, R. *Chem. Phys. Lett.* **1993**, *204*, 543.

(5) (a) David, D.; Bar, I.; Rosenwaks *J. Chem. Phys.* **1993**, *99*, 4218. (b) David, D.; Bar, I; Rosenwaks *J. Photochem. Photobiol. A* **1994**, *80*, 23.

(6) Rohrer F.; Stuhl, F. *J. Chem. Phys.* **1988**, *88*, 4788.

(7) (a) Gericke, K.-H.; Theinl R.; Comes, F. J. *J. Chem. Phys.* **1990**, *92*, 6548. (b) Gericke, K.-H.; Theinl, R.; Comes, F. J. *Chem. Phys. Lett.* **1989**, *164*, 605.

(8) Chu, J. J.; Marcus P.; Dagdigian, P. J. *J. Chem. Phys.* **1990**, *93*, 257.

(9) (a) Baronavski, A. P.; Miller, R. G.; McDonald, J. R. *Chem. Phys.* **1978**, *30*, 119. (b) Hawley, M.; Baronavski, A. P.; Nelson, H. H. *J. Chem. Phys.* **1993**, *99*, 2638.

(10) Gericke, K.-H.; Haas, T.; Lock, M.; Theinl, R.; Comes, F. J. *J. Phys. Chem.* **1991**, *95*, 6104.

(11) (a) Gericke, K.-H.; Lock, M.; Comes, F. J. *Chem. Phys. Lett.* **1991**, *186*, 427. (b) Haas, T.; Gericke, K.-H.; Maul, C.; Comes, F. J. *Chem. Phys. Lett.* **1993**, *202*, 108.

(12) Carlotti, M.; DiLonardo, D.; Galloni, G.; Trombetti, A. *Trans. Faraday Soc.* **1971**, *67*, 2852.

(13) Moore C. B.; Rosengren K. *J. Chem. Phys.* **1966**, *44*, 4108.

(14) Halligan, D. T. Ph.D Thesis, Rice University, Houston, Texas **1988**.

(15) (a) Casassa, M. P.; Foy, B. R.; Stephenson, J. C.; King, D. S. *J. Chem. Phys.* **1991**, *94*, 250. (b) Foy, B. R.; Casassa, M. P.; Stephenson, J. C.; King, D. S. *J. Chem. Phys.* **1990**, *92*, 2782. (c) Foy, B. R.; Casassa, M. P.; Stephenson, J. C.; King, D. S. *J. Chem. Phys.* **90**, 7037(1989).

(16) (a) Alexander, M. H.; Werner, H. J.; Hemmer, T.; Knowles, P. J. *J. Chem. Phys.* **1990**, *93*, 3307. (b) Alexander, M. H.; Werner, H. J.; Dagdigian, P. J. *J. Chem. Phys.* **1988**, *89*, 1388.

(17) Meier U.; Staemmler, V. *J. Phys. Chem.* **1991**, *95*, 6111.

(18) (a) Sinha, A.; Coleman, J.; Barnes R. *J. Phys. Chem.* **1994**, *98*, 12462. (b) Sinha, A.; Lock, M.; Barnes, R.; Coleman, J. *Proc. SPIE-Int. Soc. Opt. Eng.* **1995**, *205*, 2548. (c) Lock, M.; Barnes, R.; Sinha, A. *J. Chem. Phys.* **1996**, *104*, 1350. (d) Barnes, R. J.; Lock, M.; Sinha, A. *J. Phys. Chem.* **1996**, *100*, 453. (e) Lock, M.; Barnes, R. J.; Sinha, A. *J. Phys. Chem.* **1996**, *100*, 7972.

(19) (a)Brourard, M.; Martinez, M. T.; O'Mahony, J.; Simons, J. P. *Mol. Phys.* **1990**, *71*, 1021. (b) Orr-Ewing, A. J.; Simpson, W. R.; Rakitzis, T. P.; Zare, R. N. *Isr. J. Chem.* **1994**, *34*, 95. (c) Zare, R. N. *Ber. Bunsen-Ges. Phys. Chem.* **1982**, *86*, 422. (d) Zhang, J.; Riehn, C. W.; Dulligan, M.; Wittig, C. *J. Chem. Phys.* **1996**, *104*, 7027.

(20) The β_{vj} value presented is based on a global fit of Doppler profiles for the P(7) and Q(7) lines taken under several different geometries, not just the geometry shown in Figure 4a.